Chinese Journal of Aeronautics, (2018), 31(1): 137–147

Chinese Society of Aeronautics and Astronautics
& Beihang University

Chinese Journal of Aeronautics

cja@buaa.edu.cn
www.sciencedirect.com

Joint TDOA, FDOA and differential Doppler rate estimation: Method and its performance analysis

Dexiu HU [a,b], **Zhen HUANG** [a,*], **Shangyu ZHANG** [a], **Jianhua LU** [a]

[a] *Space Technology Research Center, Tsinghua University, Beijing 100084, China*
[b] *Zhengzhou Information Technology Institute, Zhengzhou 450002, China*

Received 21 November 2016; revised 10 January 2017; accepted 17 March 2017
Available online 14 November 2017

KEYWORDS

Differential Doppler rate;
Frequency difference of arrival;
Passive location;
Performance analysis;
Time difference of arrival

Abstract Considering the estimation accuracy reduction of Frequency Difference of Arrival (FDOA) caused by relative Doppler companding, a joint Time Difference of Arrival (TDOA), FDOA and differential Doppler rate estimation method is proposed and its Cramer-Rao low bound is derived in this paper. Firstly, second-order ambiguity function is utilized to reduce the dimensionality and estimate initial TDOA and differential Doppler rate. Secondly, the TDOA estimation is updated and FDOA is obtained using cross ambiguity function, in which relative Doppler companding is compensated by the existing differential Doppler rate. Thirdly, differential Doppler rate estimation is updated using cross estimator. Theoretical analysis on estimation variance and Cramer-Rao low bound shows that the final estimation of TDOA, FDOA and differential Doppler rate performs well at both low and high signal–noise ratio, although the initial estimation accuracy of TDOA and differential Doppler rate is relatively poor under low signal–noise ratio conditions. Simulation results finally verify the theoretical analysis and show that the proposed method can overcome relative Doppler companding problem and performs well for all TDOA, FDOA and differential Doppler rate estimation.

1. Introduction

In several areas including passive radar, sonar, communications, etc., the signal received by two observation sensors often contains corresponding parameters such as Time Difference of Arrival (TDOA), Frequency Difference of Arrival (FDOA), etc., which carry the information of the relative range and velocity for the target. Many practical applications can be realized using these parameters. In passive location for instance, two satellites or aircraft can locate emitter sources using time and frequency difference.[1,2] One class of source location methods are based on TDOA/FDOA.[3–7] The estimation accuracy of these parameters can be very important in these applications.

The estimation of TDOA and FDOA has been intensively studied in the past many years. For TDOA estimation, a lot of methods based on cross-correlation have been developed.[8] To further improve its accuracy, interpolation algorithms

* Corresponding author.
E-mail address: huangzhen@tsinghua.edu.cn (Z. HUANG).
Peer review under responsibility of Editorial Committee of CJA.

Production and hosting by Elsevier

https://doi.org/10.1016/j.cja.2017.11.005

and window functions[9,10] can be utilized. As the estimation of FDOA can be viewed as a dual problem of time delay estimation, it does not attract so mush interest. The problem of joint TDOA/FDOA estimation, however, is widely studied.[11–15] Cross Ambiguity Function (CAF) may be the most well-known method in this area,[12,13] although other modified methods also have been presented for some special cases, such as non-stationary higher order cumulant for correlative noises.[16] These methods model TDOA and FDOA to be constant parameters over the correlation aperture time.[11] Under this model assumption, the CAF method works well.

However, there is a contradiction between the estimation accuracy and model assumption using CAF. According to the estimation accuracy,[13] it is very important to enlarge correlation aperture time T in cross ambiguity function for a better parameter estimation accuracy and location performance. When T becomes large, however, other problems will happen. Time and frequency differences can be no more viewed as constant in this condition. Namely, Relative Time Companding (RTC) and Relative Doppler Companding (RDC) effects would deteriorate estimation accuracy distinctly.[17,18] This is because these two types of companding would not only reduce the output Signal-Noise Ratio (SNR), but also produce distortion on the shape of CAF. Specifically, RTC is mainly related to time difference and RDC is mainly related to frequency difference. The influence of these two types of companding should be discriminatively considered for different types of signals in passive location.For wideband signal, such as the wireless video or other data signals whose bandwidth is many MHz or more, RTC problem has to be mainly concerned. This is because wideband signal has a fairly high time delay resolution and relative time companding would be very sensitive relatively. Ref.[19] has analyzed the effects of RTC on time delay estimation and given the decreasing factor on the accuracy of time delay by $\Omega(\pi\dot{R}BT/c)/3$, where $\Omega(x) = |x^3(\sin x - x\cos x)^{-1}|$, $\dot{R}$ is relative velocity, T is the correlation aperture time c is the light velocity and B is signal bandwidth. This factor is useful for the case of $\dot{R}BT/c \leqslant 4$. For the case of $\dot{R}BT/c > 4$, the TDOA accuracy decreases drastically and the CAF method would become invalid. Many works have been published to solve the RTC problem, such as short-CAFs[20] and maximum likelihood correlator.[21]

For narrowband signal, such as the tactical radio signal whose bandwidth is only several kHz, however, RDC problem has to be mainly concerned. TDOA accuracy is relatively low and it needs an accurate FDOA estimation to ensure the location accuracy. In this way, it needs a much larger T compared with wideband signal, which results in a higher FDOA resolution. As a consequence, the change of FDOA would be more obvious and RDC problem is more likely to happen in this condition.[22] Since the frequency difference is dual with time difference, the decreasing factor for TDOA can be also used for FDOA, which can be given by $\Omega(\pi\ddot{R}T^2/\lambda)/3$, where $\ddot{R}$ denotes relative acceleration and λ denotes wavelength. Similarly, this factor is useful for the case of $\ddot{R}T^2/\lambda \leqslant 4$. Otherwise, the FDOA accuracy decreases drastically and the CAF method would become invalid.

To deal with RDC problem, differential Doppler rate has to be considered,[22] because the companding is caused by it. Therefore, the joint estimation of TDOA, FDOA and differential Doppler rate is needed. Compared with conventional estimation of differential time and frequency, the additional parameter of differential Doppler rate is included. It can be used to not only compensate relative Doppler companding, but also supply a new measurement for passive location.[23–25] Ref.[23] has shown that the location accuracy increases significantly by using additional parameter of differential Doppler rate.

The estimation of TDOA, FDOA and differential Doppler rate is a high-order problem for maneuvering target passive location. For the similar problem of maneuvering target detection and high-order target motion parameter estimation in active radar area, Refs.[26–28] proposed Radon-Fourier transform and generalized Radon-Fourier transform method. Besides, Refs.[29–31] also modeled radar target as fast high-order maneuvering mode and proposed fast calculation methods including the fast implementation of RFT, the Chirp-Z transform based method and particle swarm optimization. All these methods have obtained excellent results for high-order maneuvering target parameter estimation in radar area. Unfortunately, the joint estimation of TDOA, FDOA and differential Doppler rate in passive location area has not been studied comprehensively yet.

Motivated by the above facts in narrowband signal location, this paper focuses on the joint estimation of TDOA, FDOA and differential Doppler rate. We shall introduce a joint estimation method, derive the CRLB and analyze the performance of the method. The contribution of the paper includes:

(1) An estimation method for joint TDOA, FDOA and differential Doppler rate is proposed. This joint estimation is a three-dimensional problem and consequently has to be solved efficiently. Besides, the estimation accuracy is very important in this problem. To solve the above two difficulties, a three-step estimation method is proposed in this paper. The first step obtains an initial estimation of TDOA and differential Doppler rate. The second step obtains the estimation of FDOA and updates the estimation of TDOA. The third step updates differential Doppler rate estimation.
(2) The CRLB for the joint estimation is derived. The CRLB is useful to evaluate parameter estimation accuracy and forecast location precision. The derivation of CRLB is quite complicated as the source signal is unknown and non-cooperative.
(3) The performance of the proposed method is analyzed. The estimation variance of differential Doppler rate obtained by the first step is derived and compared with CRLB, showing that the variance cannot reach its CRLB in low SNR condition. Therefore, differential Doppler rate is updated in the following step and its accuracy reaches its CRLB finally.

The remainder of this paper is organized as follows. The signal model is introduced in Section 2, the proposed method is described in Section 3, the CRLB is given in Section 4, and the simulation is shown in Section 5. Finally, a brief conclusion is given in Section 6.

2. Signal model

2.1. RDC problem

The conventional estimation model of TDOA/FDOA is usually constructed as

$$\begin{cases} s_1(t) = s(t) + n_1(t) & -T/2 \leqslant t \leqslant T/2 \\ s_2(t) = s(t-\tau)\mathrm{e}^{\mathrm{j}2\pi f_c t + \mathrm{j}\varphi} + n_2(t) \end{cases} \tag{1}$$

where $s(t)$ is the source signal, T the correlation aperture time, φ the initial phase, τ the time difference, and f_c the FDOA. $n_1(t) \sim N(0, \sigma_1^2)$ and $n_2(t) \sim N(0, \sigma_2^2)$ are additive, independent white Gaussian noises. Clearly, the FDOA is assumed to be constant in this model and the differential Doppler rate is ignored. Under this model assumption, the estimation accuracy of TDOA and FDOA using CAF can be given respectively as[13]

$$\sigma_\tau \approx \frac{1}{\beta_s} \times \frac{1}{\sqrt{B_n T r}} \tag{2a}$$

$$\sigma_f \approx \frac{0.55}{T} \times \frac{1}{\sqrt{B_n T r}} \tag{2b}$$

where B_n denotes noise bandwidth of the receiver, β_s "RMS radian frequency" of the signal, and r equivalent signal-noise rate. Note that

$$\beta_s^2 = \frac{\int_{-\infty}^{\infty} (2\pi f)^2 G(f) \mathrm{d}f}{\int_{-\infty}^{\infty} G(f) \mathrm{d}f} \tag{3a}$$

$$\frac{1}{r} = \frac{1}{2}\left(\frac{1}{r_1} + \frac{1}{r_2} + \frac{1}{r_1 r_2}\right) \tag{3b}$$

where $G(f)$ is the power spectral density of $s(t)$ and r_i the SNR of $s_i(t), \quad i = 1, 2$.

In practice, RTC and RDC problem may affect the TDOA/FDOA estimation performance. For wideband signal, such as the video and data signals with the bandwidth of several MHz, the relative time companding has to be mainly concerned. The time resolution of TDOA is $1/B$, where B denotes the bandwidth of received signal. Given a certain integration time T, the time companding during this time is $f_c/f_0 T$, where f_0 denotes carrier frequency. Therefore, the relative time companding factor is $f_c/f_0 BT$. Ref.[20] has shown that when $f_c/f_0 BT$ exceeds 2.8, the relative time companding effect has to be considered. As wideband signal has much higher B, the relative time companding is more likely to happen. For example, when the carrier frequency is 400 MHz, the FDOA 2000 Hz, the bandwidth 10 MHz and the integration time 0.1 s, the relative time companding factor achieves 5 and has to be concerned in practice.

For narrowband signal, such as the tactical radio signal with bandwidth of several kHz, however, relative time companding is not likely to happen. For the same condition of the above example, when bandwidth is 10 kHz, the relative time companding factor is only 0.005, which can be ignored. As the time delay estimation accuracy is very low for narrowband signal, it needs a considerable FDOA accuracy to ensure location accuracy. As indicated by Eq. (2b), the only way to improve FDOA accuracy is to enlarge T. The influence of a larger T can be described in two aspects. On the one hand, a larger T means a higher FDOA resolution, as it deserves $1/T$. On the other hand, the Doppler companding is more distinct. We define a relative Doppler companding factor γ as

$$\gamma = \ddot{R}T^2/\lambda = \dot{f}_c T^2 \tag{4}$$

where $\ddot{R}$ is the relative acceleration, λ is the wavelength, and $\dot{f}_c = \ddot{R}/\lambda$ is the differential Doppler rate. It can be found that γ is a normalized factor to signify the ratio of Doppler companding with respect to FDOA resolution. When $\gamma = 2$ for instance, it means that Doppler companding is two times as much as FDOA resolution.

Fig. 1 shows the RDC effect related to Doppler companding factor γ. Note that the integral time is normalized to 1 s. It plots curves of conventional CAF slices in the direction of FDOA. (A) When $\gamma = 0$, namely $\dot{f}_c = 0$, the signal model assumed in CAF is exactly the same as real signal model. Under this condition, the output gain is the highest and the CAF shape is the narrowest. (B) When $\dot{f}_c$ enlarges, such as $\gamma = 1, 2, 3$, the output gain declines while the shape of CAF becomes wider. (C) When $\dot{f}_c$ further enlarges, such as $\gamma = 4, 5$, both the output gain and shape of CAF deteriorate seriously; under this condition, the CAF has no obvious peak and it fails to estimate FDOA.

For some particular scenario such as rotating tethered satellite formation,[32] the differential Doppler rate $\dot{f}_c$ itself is huge. Meanwhile, the desired correction aperture time length is also quite long for the narrowband signal. This will result in a large γ. For instance, when $\dot{f}_c = 20$ Hz/s and $T = 0.5$ s, γ achieves 5 and CAF fails to estimate FDOA in this condition. Thus, for a better FDOA and source location accuracy, differential Doppler rate has to be considered and RDC has to be avoided. What's more, the differential Doppler rate parameter can also be used as a location parameter.

2.2. Dynamic signal model

The RDC problem occurs due to the ignoring of differential Doppler rate and the inconsistence between the assumed signal model and the real one. We reconstruct the signal model as

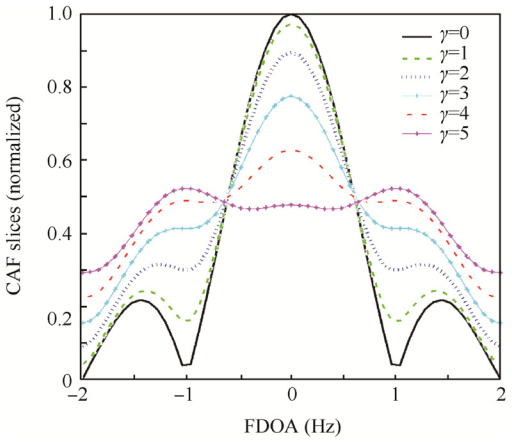

Fig. 1 FDOA distortion of CAF with respect to Doppler companding factor γ.

$$\begin{cases} s_1(t) = s(t) + n_1(t) & -T/2 \leqslant t \leqslant T/2 \\ s_2(t) = s(t-\tau)\mathrm{e}^{\mathrm{j}2\pi(f_c t + 0.5\dot{f}_c t^2)+\mathrm{j}\varphi} + n_2(t) \end{cases} \tag{5}$$

where $n_1(t) \sim N(0, \sigma_1^2)$ and $n_2(t) \sim N(0, \sigma_2^2)$ are independent Gaussian noises. Note that $s(t)$ is power normalized in this model and SNRs of $s_1(t)$ and $s_2(t)$ are hence $1/\sigma_1^2$ and $1/\sigma_2^2$, respectively. Compared with conventional model in Eq. (1), the FDOA is dynamic and differential Doppler rate $\dot{f}_c$ is considered in this model. It has to be noted that the model used in CAF can be viewed as a special case of the new model when $\dot{f}_c = 0$.

As the TDOA, FDOA and differential Doppler rate are all unknown in the model, it has to concentrate on the joint estimation of all these parameters. After uncomplicated deduction, the correlation estimator, which is also Maximum Likelihood (ML) estimator, can be given as

$$\begin{cases} (\hat{\tau}, \hat{f}_c, \hat{\dot{f}}_c) = \arg\max_{\tau, f_c, \dot{f}_c} |C(\tau, f_c, \dot{f}_c)| \\ C(\tau, f_c, \dot{f}_c) = \int_{-T/2}^{T/2} s_1^*(t) s_2(t+\tau)\mathrm{e}^{\mathrm{j}2\pi(f_c t + 0.5\dot{f}_c t^2)}\mathrm{d}t \end{cases} \tag{6}$$

However, this estimator is very computationally expensive, because it needs a three-dimensional searching. This paper seeks other alternative solution for joint estimation of TDOA, FDOA and differential Doppler rate.

3. Proposed estimation method

Since the joint estimation of TDOA, FDOA and differential Doppler rate needs a three-dimensional searching, it is very computationally expensive. So parameter dimension reduction method is needed. This section tries to decrease the parameter dimension using the Second-order Ambiguity Function (SAF) and estimate the parameters iteratively.

3.1. Preparation of proposed method

The high-order ambiguity function[33–35] is widely used to estimate parameters of Polynomial-Phase Signal (PPS) embedded in noise. As only second-order is used in the proposed method, this subsection briefly introduces this specific algorithm.

A second-order PPS is given with

$$s(n) = A\mathrm{e}^{\mathrm{j}2\pi(a_0 + a_1 n + a_2 n^2)} \tag{7}$$

where A denotes the amplitude, and a_0, a_1 and a_2 denote the coefficient of different orders. For a certain time lag l, the Second-order Instantaneous Moment (SIM) of $s(n)$ can be given as

$$\begin{aligned} x^l(n) &= s(n+l)s^*(n-l) \\ &= A^2\mathrm{e}^{\mathrm{j}2\pi(2a_1 l + 4a_2 l n)} \end{aligned} \tag{8}$$

The SAF is defined as the discrete Fourier transform of the SIM, namely

$$\mathrm{SAF}(f; l) = \sum_{n=-N/2}^{N/2} x^l(n)\mathrm{e}^{-\mathrm{j}2\pi f n} \tag{9}$$

It can be found from Eq. (8) that $x^l(n)$ is a sinusoid. Therefore, the corresponding SAF transform in Eq. (9) has a peak value at the frequency of

$$f = 4a_2 l \tag{10}$$

This characteristic inspires us that the FDOA can be eliminated and the parameter dimension can be decreased using SAF.

3.2. Dimensionality reduction using SAF

When considering the TDOA, FDOA and differential Doppler rate simultaneously, the discretely sampled signals can be given according to Eq. (5) as

$$\begin{cases} s_1(n) = s(n) + n_1(n) & -N/2 \leqslant n \leqslant N/2 \\ s_2(n) = s(n-\tau)\mathrm{e}^{\mathrm{j}2\pi(f_d n + 0.5\dot{f}_d n^2)+\mathrm{j}\varphi} + n_2(n) \end{cases} \tag{11}$$

Note that $f_d = f_c T_s$ and $\dot{f}_d = \dot{f}_c T_s^2$ are normalized parameters. We use SAF transform here to decrease the dimensionality of unknown parameters.

As beginning, the cross-conjugate product of the two received signals can be given as

$$\begin{aligned} z_m(n) &= s_1^*(n)s_2(n+m) \\ &= z_{0m}(n) + v'(n) \end{aligned} \tag{12}$$

where

$$z_{0m}(n) = s^*(n)s(n-\tau+m)\mathrm{e}^{\mathrm{j}2\pi(f_d(n+m)+0.5\dot{f}_d(n+m)^2)+\mathrm{j}\varphi} \tag{13}$$

and $v'(n)$ is the noise. Then, for a certain time lag l, the SIM transform of $z_m(n)$ can be given as

$$x_m^l(n) = x_{0m}^l(n) + v''(n) \tag{14}$$

where $x_{0m}^l(n)$ is the SIM transform of $z_{0m}(n)$, and $v''(n)$ the noise. $z_{0m}(n)$ and $x_{0m}^l(n)$ can be further discussed in the following two aspects, assuming $s(n)$ being envelope-constant.

Case 1. $m = \tau$. In this condition,

$$z_{0m}(n) = s^*(n)s(n)\mathrm{e}^{\mathrm{j}2\pi(f_d(n+m)+0.5\dot{f}_d(n+m)^2)} \tag{15}$$

Obviously, $z_{0m}(n)$ is a second-order PPS signal and $z_m(n)$ is its noised form. Furthermore,

$$x_{0m}^l(n) = |s(n)s^*(n)|^2\mathrm{e}^{\mathrm{j}2\pi(2\dot{f}_d l n)+\mathrm{j}\varphi_0} \tag{16}$$

with φ_0 being a fixed value with respective to n. It can be found that $x_{0m}^l(n)$ is a sine. Therefore, $x_m^l(n)$ is a noised sine and its corresponding SAF has a peak value at $f = 2\dot{f}_d l$ according to Eq. (10).

Case 2. $m \neq \tau$. We suppose that the instantaneous phase of $s(n)$ is $p(n)$, which is a random value for phase modulated signal, and then $z_{0m}(n)$ can be expressed as

$$z_{0m}(n) = |s(n)s^*(n-\tau+m)|\mathrm{e}^{\mathrm{j}2\pi(f(n+m)+0.5\dot{f}(n+m)^2)+\mathrm{j}\varphi}\mathrm{e}^{\mathrm{j}(p(n+m)-p(n))} \tag{17}$$

It can be found that $z_{0m}(n)$ is not a second-order PPS, because the item $p(n+m) - p(n)$ is random. As a result, $x_{0m}^l(n)$ is not a sine signal and its corresponding SAF is colorlessly distributed, with no obvious peak anywhere.

In conclusion, when $\tau = m$, the SAF transform of $z_m(n)$ has a peak at $f = 2\dot{f}_d l$. Otherwise, there is no obvious peak in the SAF. Namely, for different combinations of m and f, only when $m = \tau$ and $f = 2\dot{f}_d l$, there is a peak. The SAF can be viewed as power distribution of cross-conjugate product of $s_1(n)$ and $s_2(n)$ with respect to TDOA and differential Doppler

rate. When $m=\tau$ and $f=2\dot{f}_{\mathrm{d}}l$, the power is gathered. Otherwise, the power is dispersed. In this way, the SAF supplies a good tool to eliminate initial FDOA and reduce the parameter dimensionality from the three-dimension of TDOA, FDOA and differential Doppler rate to the two-dimension of TDOA and differential Doppler rate.

Furthermore, the following issues have to be discussed: (A) The selection of l for a better estimation performance. (B) The estimation variance using SAF. (C) The way to estimate initial FDOA. We shall discuss the selection of l, the variance of differential Doppler rate, compare it with its CRLB and modify the estimation strategy according to the comparison. After that, the final processing flow of the proposed method can be given.

3.3. Resolution of Doppler rate and selection of l

According to the expression of $x_{0m}^{l}(n)$, the resolution of $\dot{f}_{\mathrm{c}}$ can be given as[34]

$$\Delta\dot{f}_{\mathrm{c}}=\frac{1}{2MlT_{\mathrm{s}}^{2}}=\frac{1}{2(N-2l)lT_{\mathrm{s}}^{2}} \tag{18}$$

where T_{s} denotes the sample interval and M the length of $x_{m}^{l}(n)$. According to the definition of $x_{m}^{l}(n)$, we have $M=N-2l$.

It is clear that the differential Doppler rate resolution is related to l. Both a too big l and a too small l would result in a low resolution. The best selection of l should optimize differential Doppler rate resolution, thus maximizing $(N-2l)l$, because the differential Doppler rate is not too large in practice. It is not hard to conclude that when $l=N/4$, $(N-2l)l$ is the largest and the resolution of differential Doppler rate is the best. So, the selection of l should be $N/4$ in practice. The resolution of differential Doppler rate in this condition yields

$$\Delta\dot{f}_{\mathrm{c}}=\frac{4}{T^{2}} \tag{19}$$

Eq. (19) also supplies a law for the correction time T for differential Doppler rate estimation. To estimate Doppler effectively, T has to satisfy $T\geqslant\sqrt{4/\dot{f}_{\mathrm{c}}}$. Namely, to estimate and apply differential Doppler rate effectively, the correction time should be large enough.

3.4. Estimation variance using SAF

This subsection discusses the estimation variance of TDOA and differential Doppler rate using SAF.

For a certain time lag l, $x_{m}^{l}(n)$ can be rewritten according to Eq. (14) as

$$\begin{aligned}x_{m}^{l}(n)&=z_{m}(n+l)z_{m}^{*}(n-l)\\&=s_{1}^{*}(n+l)s_{2}(n+m+l)s_{1}(n-l)s_{2}^{*}(n+m-l)\\&=s^{*}(n+l)s(n-l)s(n+l-\tau+m)s^{*}(n-l-\tau+m)\mathrm{e}^{\mathrm{j}2\pi(2\dot{f}_{\mathrm{d}}ln)}\\&\quad+\mathrm{j}\varphi_{0}+v''(n)\end{aligned} \tag{20}$$

where φ_0 is a fixed value with respect to n and $v''(n)$ the noise. We define the following variables as

$$\begin{cases}a(n)=s^{*}(n+l)s(n-l)\\a_{1}(n)=s_{1}^{*}(n+l)s_{2}(n-l)=a(n)+v_{1}'(n)\\a_{2}(n)=s_{1}^{*}(n+l-\tau)s_{2}(n-l-\tau)\mathrm{e}^{\mathrm{j}2\pi(2\dot{f}_{\mathrm{d}}ln)+\mathrm{j}\varphi_{0}}\\\quad=a(n-\tau)\mathrm{e}^{\mathrm{j}2\pi(2\dot{f}_{\mathrm{d}}ln)+\mathrm{j}\varphi_{0}}+v_{2}'(n)\end{cases} \tag{21}$$

Therefore, $x_{m}^{l}(n)$ can be rewritten as

$$\begin{aligned}x_{m}^{l}(n)&=a(n)a(n-\tau+m)\mathrm{e}^{\mathrm{j}2\pi(2\dot{f}_{\mathrm{d}}ln)+\mathrm{j}\varphi_{0}}+v''(n)\\&=a_{1}(n)a_{2}(n+m)\end{aligned} \tag{22}$$

It can be seen from Eqs. (20)–(22) that the SAF of $s_1(n)$ and $s_2(n)$ can be also viewed as conventional CAF of $a_1(n)$ and $a_2(n)$. Therefore, the estimation accuracy of TDOA and differential Doppler rate can be directly given by CAF method,[13] which can be expressed as

$$\mathrm{var}(\tau)=\frac{1}{\beta_{\mathrm{as}}^{2}B_{\mathrm{n}}T_{\mathrm{a}}r_{\mathrm{a}}} \tag{23a}$$

$$\mathrm{var}(\dot{f}_{\mathrm{c}})=\frac{\mathrm{var}(2lT_{\mathrm{s}}\dot{f}_{\mathrm{c}})}{(2lT_{\mathrm{s}})^{2}}=\frac{1}{(2lT_{\mathrm{s}})^{2}}\frac{3}{\pi^{2}T_{\mathrm{a}}^{3}B_{\mathrm{n}}r_{\mathrm{a}}} \tag{23b}$$

where β_{as} denotes the rms bandwidth of $a(n)$, $T_{\mathrm{a}}=(N-2l)T_{\mathrm{s}}$ denotes the time length of $a(n)$, and

$$\frac{1}{r_{\mathrm{a}}}=\frac{1}{2}\left(\frac{1}{r_{\mathrm{a1}}}+\frac{1}{r_{\mathrm{a2}}}+\frac{1}{r_{\mathrm{a1}}r_{\mathrm{a2}}}\right) \tag{24}$$

Note that r_{a1} and r_{a2} denote the SNR of $a_1(n)$ and $a_2(n)$, respectively. As $s(t)$ is power normalized in the signal model, we have

$$\frac{1}{r_{\mathrm{a1}}}=\frac{1}{r_{\mathrm{a2}}}=\sigma_{v'}^{2}=\sigma_{1}^{2}+\sigma_{2}^{2}+\sigma_{1}^{2}\sigma_{2}^{2} \tag{25}$$

To achieve the best differential Doppler rate resolution, l is assigned to be $N/4$. In this condition, Eqs. (23a) and (23b) can be simplified as

$$\mathrm{var}(\tau)=\frac{2}{\beta_{\mathrm{as}}^{2}}\times\frac{1}{B_{\mathrm{n}}T}\times\frac{\sigma_{v''}^{2}}{2} \tag{26a}$$

$$\mathrm{var}(\dot{f}_{\mathrm{c}})=\frac{3\times2^{5}}{\pi^{2}T^{4}}\times\frac{1}{B_{\mathrm{n}}T}\times\frac{\sigma_{v''}^{2}}{2} \tag{26b}$$

where $\sigma_{v''}^{2}=2\sigma_{v'}^{2}+\sigma_{v'}^{4}$. As the estimation variance and CRLB of differential Doppler rate are both obtained in this paper, they can be compared as follows:

$$\eta=\frac{\mathrm{var}(\dot{f}_{\mathrm{c}})}{\mathrm{CRLB}(\dot{f}_{\mathrm{c}})}=\frac{96}{180}\times\frac{\sigma_{v''}^{2}}{\sigma_{1}^{2}+\sigma_{2}^{2}} \tag{27}$$

Let's discuss this η under the conditions of high SNR and low SNR.

(1) At high SNR, σ_1 and σ_2 are very small and the cross terms of σ_1 and σ_2 can be viewed as higher-order small items. Therefore, $\sigma_{v''}^{2}\approx2(\sigma_{1}^{2}+\sigma_{2}^{2})$ and $\eta\approx1.07$. This means that the estimation of differential Doppler rate using SAF can approach CRLB at high SNR.

(2) At low SNR, the cross terms of σ_1 and σ_2 enlarge noises dramatically and η should be much larger than 1. This means that the estimation variance of differential Doppler rate cannot reach its CRLB. Besides, the accuracy of TDOA estimation using SAF cannot reach its CRLB in the same way that the cross terms of σ_1 and σ_2 enlarge

noises dramatically at low SNR. The above problems at low SNR occur mainly because the SAF transform enlarges the noises.

3.5. Processing flow

To improve the accuracy of differential Doppler rate and TDOA, especially at low SNR, we have to reconsider the estimation method and try to decrease the cross items. Besides, the estimation of FDOA has to be considered.

Firstly, we concentrate on the TDOA and FDOA estimation. As the initial differential Doppler rate has been obtained using SAF, the RDC can be compensated. In this way, TDOA can be updated and FDOA can be obtained using CAF after differential Doppler rate compensation, namely

$$\begin{cases} (\hat{\tau},\hat{f}_c) = \arg\max_{\tau,f_c}|\mathrm{CAF}(\tau,f_c)| \\ \mathrm{CAF}(\tau,f_c) = \int_{-T/2}^{T/2} s_1^*(t)s_2(t+\tau)\mathrm{e}^{-\mathrm{j}2\pi(f_c t+0.5\hat{\dot{f}}_c t^2)}\mathrm{d}t \end{cases} \tag{28}$$

where $\hat{\dot{f}}_c$ is the initial differential Doppler rate estimation using SAF. Compared with the conventional CAF estimator, this estimator is different in the RDC compensation. FDOA companding can be avoided and FDOA estimation is no more affected by RDC problem. Compared with the TDOA estimator using SAF, the cross items of this estimator are much less. As a result, the estimation accuracy of TDOA can be improved much, approaching its CRLB.

Then, we concentrate on the accurate estimation of differential Doppler rate and try to improve its accuracy at low SNR. The differential Doppler rate can be iterated using the estimation of TDOA and FDOA, namely

$$\hat{\dot{f}}_c = \arg\max_{\dot{f}_c}\left|\int_{-T/2}^{T/2} s_1^*(t)s_2(t+\hat{\tau})\mathrm{e}^{\mathrm{j}2\pi(\hat{f}_c t+0.5\dot{f}_c t^2)}\mathrm{d}t\right| \tag{29}$$

where $\hat{f}_c$ and $\hat{\tau}$ denote the estimated time delay and frequency difference. This method uses cross-estimator and reduces cross items compared with SAF. Thus, the accuracy of differential Doppler rate can be increased much. It has to be noted that the iterated estimation of differential Doppler rate is not essential if this parameter is not used in passive location. However, if one wants to improve location accuracy by using additional parameter of differential Doppler rate, this step is needed.

The final method for joint TDOA, FDOA and differential Doppler rate estimation can be obtained from above analyses, which is listed in Table 1. The proposed method includes three steps. The first step obtains an initial estimation of TDOA and differential Doppler rate using SAF transform, which can reduce dimension of parameter space. The second step uses CAF with differential Doppler rate compensation to update TDOA estimation and obtain FDOA estimation. The TDOA searching scope in this step can be narrower than that in the first step, because the initial TDOA estimation is known. The third step of the proposed method is to update the estimation of differential Doppler rate using cross estimator, which introduces less cross items.

The computation amount of the proposed method is much smaller than that of ML estimator given by Eq. (6). We suppose that the date length is N, TDOA searching number is N_t, TDOA searching number is N_f and differential Doppler rate searching number is N_{df}. The ML estimator's computation amount is approximately $NN_tN_fN_{df}$, while that of the proposed method is approximately $2NN_tN_{df} + NN_tN_f + NN_f$, where the three addition items are the computation amount in the three steps. If $N_t = 100$, $N_f = 100$ and $N_{df} = 100$, the computation burden of the proposed method is only 3% of ML estimator. Therefore, the computation burden decreases obviously.

Table 1 Steps of proposed method.

Step 1. initial estimation of TDOA and differential Doppler rate using SAF
  For $m = \tau_{min} : \tau_{max}$
    calculate the cross-conjugate product of $s_1(n)$ and $s_2(n)$
    For $\dot{f}_c = \dot{f}_{cmin} : \dot{f}_{cmax}$
      calculate SAF of the cross-conjugate product
    End
  End
  obtain TDOA estimation $\hat{\tau}$ and differential Doppler rate estimation $\hat{\dot{f}}_c$ using SAF
Step 2. joint estimation of TDOA and FDOA using Eq. (28)
  For $\tau = \tau_{min} : \tau_{max}$ and $f_c = f_{cmin} : f_{cmax}$
    calculate CAF(τ, f_c) with differential Doppler rate compensation of $\hat{\dot{f}}_c$
  End
  Update TDOA estimation $\hat{\tau}$ and obtain FDOA estimation $\hat{f}_c$ using CAF
Step 3. update differential Doppler rate estimation using cross estimator using Eq. (29).

Note that τ_{max} and τ_{min} denote the largest and least possible value of TDOA, f_{cmax} and f_{cmin} denote the largest and least possible value of FDOA, and $\dot{f}_{cmin}$ and $\dot{f}_{cmax}$ denote the largest and least possible value of differential Doppler rate.

For the sake of completeness, we discuss the error propagation characteristic of the proposed method here. First, we focus on the influence of differential Doppler rate error on TDOA/FDOA estimation. In the second step, the estimated differential Doppler rate is used to compensate the relative Doppler companding. According to Eq. (26b), the RMSE of differential Doppler rate estimation in the first step is

$$\delta = \frac{\sqrt{3}\times 4\sigma_{v''}}{\pi\sqrt{N}T^2} \tag{30}$$

where $N = B_nT$ is the sample number. According to Eqs. (4) and (30), the residual Doppler companding factor after compensation is approximately

$$\delta_\gamma = \delta T^2 = \frac{\sqrt{3}\times 4\sigma_{v''}}{\pi\sqrt{N}} \tag{31}$$

As the sample number N is large in most cases, the factor is very small. For example, when the SNR of received signal is 0 dB and the number of sample is 10,000, it can be calculated that the residual Doppler companding factor is 0.085. This companding factor is far smaller than 1 and will become further smaller in higher SNR condition. This factor can be ignored in the estimation of TDOA and FDOA. As a result, the accuracy of TDOA and FDOA can approach CRLB using compensated CAF. Moreover, as the TDOA and FDOA are accurate enough and have approached CRLB, the accuracy

of differential Doppler rate can be assured in the third step and this parameter can also approach CRLB consequently.

4. CRLB of joint TDOA, FDOA and Doppler rate estimation

This section concerns the CRLB of joint TDOA, FDOA and differential Doppler rate estimation.

4.1. Vector signal model

The source signal vector and its time-delayed form can be expressed using vectors as follows:

$$\begin{cases} \boldsymbol{s} \triangleq \left[s\left(-\frac{N}{2}\right), s\left(-\frac{N}{2}+1\right), \ldots, s\left(\frac{N}{2}-1\right) \right]^{\mathrm{T}} \\ \boldsymbol{s}_\tau \triangleq \left[s_\tau\left(-\frac{N}{2}\right), s_\tau\left(-\frac{N}{2}+1\right), \ldots, s_\tau\left(\frac{N}{2}-1\right) \right]^{\mathrm{T}} \end{cases} \tag{32}$$

where $s_\tau(n)$ denotes $s(n-\tau)$. It is clear that the relation $|\tau| \ll T$ is always obeyed in practice (T denotes the correlation aperture time).[15] As a result, $\boldsymbol{s}_\tau$ can be approximated as $\boldsymbol{s}_\tau \approx \boldsymbol{F}^{\mathrm{H}}\boldsymbol{D}_\tau\boldsymbol{F}\boldsymbol{s}$ using discrete Fourier transform, where

$$\begin{cases} \boldsymbol{F} = \frac{1}{\sqrt{N}} \exp\left(-\mathrm{j}\frac{2\pi}{N}\boldsymbol{n}\boldsymbol{n}^{\mathrm{T}}\right) \\ \boldsymbol{D}_\tau = \mathrm{diag}\left[\exp(-\mathrm{j}\frac{2\pi}{N}\boldsymbol{n}\tau)\right] \end{cases} \tag{33}$$

with $\boldsymbol{n} = [-N/2, -N/2+1, \ldots, N/2-1]^{\mathrm{T}}$. By substituting $\boldsymbol{s}$ and $\boldsymbol{s}_\tau$ into Eq. (11), the sampled signal vectors can be correspondingly given by

$$\begin{cases} \boldsymbol{s}_1 = \boldsymbol{s} + \boldsymbol{n}_1 \\ \boldsymbol{s}_2 = \mathrm{e}^{\mathrm{j}\varphi}\boldsymbol{D}_1\boldsymbol{D}_2\mathbf{F}^{\mathrm{H}}\boldsymbol{D}_\tau\boldsymbol{F}\boldsymbol{s} + \boldsymbol{v}_2 = \mathrm{e}^{\mathrm{j}\varphi}\boldsymbol{G}\boldsymbol{s} + \boldsymbol{n}_2 \end{cases} \tag{34}$$

where $\boldsymbol{D}_1 = \mathrm{diag}\{\exp(\mathrm{j}2\pi f_{\mathrm{d}}\boldsymbol{n})\}$, $\boldsymbol{D}_2 = \mathrm{diag}\left\{\exp(\mathrm{j}\pi\dot{f}_{\mathrm{d}}\boldsymbol{n}\odot\boldsymbol{n})\right\}$ and $\boldsymbol{G} = \boldsymbol{D}_1\boldsymbol{D}_2\boldsymbol{F}^{\mathrm{H}}\boldsymbol{D}_\tau\boldsymbol{F}$. Note that $\odot$ denotes dot cross with $(\boldsymbol{A}\odot\boldsymbol{B})_{ij} = \boldsymbol{A}_{ij}\boldsymbol{B}_{ij}$. The expression in Eq. (34) constructs the vector model of the received signal, in which the delayed signal is represented by discrete Fourier transform of original signal. Therefore, this model contains less unknown parameters than the model in Eq. (11).

4.2. Signal-specific CRLB

This subsection concentrates on the CRLB for our interested parameter $\boldsymbol{\theta} \triangleq [\tau, \varphi, f_{\mathrm{d}}, \dot{f}_{\mathrm{d}}]^{\mathrm{T}}$ with $\mathbf{s}$ unknown. To this end, a new parameter vector can be defined containing all the unknown parameters, namely $\boldsymbol{\alpha} \triangleq [\mathrm{Re}\{\boldsymbol{s}^{\mathrm{T}}\}, \mathrm{Im}\{\boldsymbol{s}^{\mathrm{T}}\}, \boldsymbol{\theta}^{\mathrm{T}}]^{\mathrm{T}} \in \mathbf{R}^{(2N+4)\times 1}$. Furthermore, the posterior probability of the observed signals $\boldsymbol{x} \triangleq [\boldsymbol{s}_1^{\mathrm{T}}, \boldsymbol{s}_2^{\mathrm{T}}]^{\mathrm{T}} \in \mathbf{C}^{2N\times 1}$ can be given as

$$p(\boldsymbol{x};\boldsymbol{\alpha}) = \frac{1}{(2\pi)^N}\frac{1}{|\boldsymbol{\Sigma}|^{1/2}}\exp\left\{-\frac{1}{2}(\boldsymbol{x}-\boldsymbol{u})^{\mathrm{H}}\boldsymbol{\Sigma}^{-1}(\boldsymbol{x}-\boldsymbol{u})\right\} \tag{35}$$

where $\boldsymbol{u}$ and $\boldsymbol{\Sigma}$ are mean and covariance matrix respectively, namely

$$\boldsymbol{u} = \begin{bmatrix} \boldsymbol{s} \\ \mathrm{e}^{\mathrm{j}\varphi}\boldsymbol{G}\boldsymbol{s} \end{bmatrix},\ \boldsymbol{\Sigma} = \begin{bmatrix} \sigma_1^2\boldsymbol{I}_N & \mathbf{0} \\ \mathbf{0} & \sigma_2^2\boldsymbol{I}_N \end{bmatrix} \tag{36}$$

The Fisher Information Matrix (FIM) of α can be given by[36]

$$\boldsymbol{J}_\alpha = 2\mathrm{Re}\left\{\left[\frac{\partial\boldsymbol{u}}{\partial\alpha}\right]^{\mathrm{H}}\boldsymbol{\Sigma}^{-1}\left[\frac{\partial\boldsymbol{u}}{\partial\alpha}\right]\right\} \tag{37}$$

$\partial\boldsymbol{u}/\partial\alpha$ can be calculated as

$$\frac{\partial\boldsymbol{u}}{\partial\alpha} = \begin{bmatrix} \boldsymbol{I}_N & \mathrm{j}\boldsymbol{I}_{\mathrm{N}} & \mathbf{0}_{\mathrm{N}\times 3} \\ \mathrm{e}^{\mathrm{j}\varphi}\boldsymbol{G}\boldsymbol{I}_{\mathrm{N}} & \mathrm{j}\mathrm{e}^{\mathrm{j}\varphi}\boldsymbol{G}\boldsymbol{I}_{\mathrm{N}} & \boldsymbol{B} \end{bmatrix} \tag{38}$$

where

$$\begin{aligned} \boldsymbol{B} &= \frac{\partial(\mathrm{e}^{\mathrm{j}\varphi}\boldsymbol{G}\boldsymbol{s})}{\partial\boldsymbol{\theta}} \\ &= \mathrm{e}^{\mathrm{j}\varphi}\left[-\mathrm{j}\boldsymbol{G}\boldsymbol{s}^{(1)}, \mathrm{j}\boldsymbol{G}\boldsymbol{s}, \mathrm{j}2\pi\boldsymbol{N}\boldsymbol{G}\boldsymbol{s}, \mathrm{j}\pi\boldsymbol{N}^2\boldsymbol{G}\boldsymbol{s}\right] \end{aligned} \tag{39}$$

Note that $\boldsymbol{N} = \mathrm{diag}\{\boldsymbol{n}\}$ and $\boldsymbol{s}^{(1)} = \frac{2\pi}{N}\boldsymbol{F}^{\mathrm{H}}\boldsymbol{N}\boldsymbol{F}\boldsymbol{s}$ in Eq. (39). Consequently, by substituting $\boldsymbol{u}$ and α into Eq. (37), the FIM of α yields

$$\boldsymbol{J}_\alpha = 2\begin{bmatrix} \left(\frac{1}{\sigma_1^2}+\frac{1}{\sigma_2^2}\right)\boldsymbol{I}_N & \mathbf{0} & \frac{1}{\sigma_2^2}\mathrm{Re}(\boldsymbol{P}) \\ \mathbf{0} & \left(\frac{1}{\sigma_1^2}+\frac{1}{\sigma_2^2}\right)\boldsymbol{I}_N & \frac{1}{\sigma_2^2}\mathrm{Im}(\boldsymbol{P}) \\ \frac{1}{\sigma_2^2}\mathrm{Re}(\boldsymbol{P}^{\mathrm{H}}) & -\frac{1}{\sigma_2^2}\mathrm{Im}(\boldsymbol{P}^{\mathrm{H}}) & \frac{1}{\sigma_2^2}\mathrm{Re}(\boldsymbol{B}^{\mathrm{H}}\boldsymbol{B}) \end{bmatrix} \tag{40}$$

where $\boldsymbol{P} = \boldsymbol{G}^{\mathrm{H}}\boldsymbol{B}$.

Up to now, the $(2N+4)\times(2N+4)$ FIM of α have been derived. However, it has to be recalled that our only interested parameter is θ. Therefore, we begin to obtain the FIM of θ from $\boldsymbol{J}_\alpha$. According to Eq. (40), it can be deduced that

$$J_\theta = 2\frac{\mathrm{Re}(\boldsymbol{B}^{\mathrm{H}}\boldsymbol{B})}{\sigma_1^2+\sigma_2^2} \tag{41}$$

where $\boldsymbol{J}_\theta$ denotes the FIM of θ. After some algebraic manipulation, the explicit expression of $\boldsymbol{B}^{\mathrm{H}}\boldsymbol{B}$ can be given in Eq. (42). This expression is related to the source signal, namely signal-specific. For different signal type and observation window, it can give a specific and accurate bound. Thus, it is fit for any type of signal.

$$\boldsymbol{B}^{\mathrm{H}}\boldsymbol{B} = \begin{bmatrix} \boldsymbol{s}^{(1)\mathrm{H}}\boldsymbol{s}^{(1)} & -\boldsymbol{s}^{\mathrm{H}}\boldsymbol{s}^{(1)} & -2\pi\boldsymbol{s}^{(1)\mathrm{H}}\boldsymbol{G}^{\mathrm{H}}\boldsymbol{N}\boldsymbol{G}\boldsymbol{s} & -\pi\boldsymbol{s}^{(1)\mathrm{H}}\boldsymbol{G}^{\mathrm{H}}\boldsymbol{N}^2\boldsymbol{G}\boldsymbol{s} \\ -\boldsymbol{s}^{\mathrm{H}}\boldsymbol{s}^{(1)} & \boldsymbol{s}^{\mathrm{H}}\boldsymbol{s} & 2\pi\boldsymbol{s}^{\mathrm{H}}\boldsymbol{G}^{\mathrm{H}}\boldsymbol{N}\boldsymbol{G}\boldsymbol{s} & 2\pi^2\boldsymbol{s}^{\mathrm{H}}\boldsymbol{G}^{\mathrm{H}}\boldsymbol{N}^2\boldsymbol{G}\boldsymbol{s} \\ -2\pi\boldsymbol{s}^{(1)\mathrm{H}}\boldsymbol{G}^{\mathrm{H}}\boldsymbol{N}\boldsymbol{G}\boldsymbol{s} & 2\pi\boldsymbol{s}^{\mathrm{H}}\boldsymbol{G}^{\mathrm{H}}\boldsymbol{N}\boldsymbol{G}\boldsymbol{s} & 4\pi^2\boldsymbol{s}^{\mathrm{H}}\boldsymbol{G}^{\mathrm{H}}\boldsymbol{N}^2\boldsymbol{G}\boldsymbol{s} & 2\pi^2\boldsymbol{s}^{\mathrm{H}}\boldsymbol{G}^{\mathrm{H}}\boldsymbol{N}^3\boldsymbol{G}\boldsymbol{s} \\ -\pi\boldsymbol{s}^{(1)\mathrm{H}}\boldsymbol{G}^{\mathrm{H}}\boldsymbol{N}^2\boldsymbol{G}\boldsymbol{s} & \pi\boldsymbol{s}^{\mathrm{H}}\boldsymbol{G}^{\mathrm{H}}\boldsymbol{N}^2\boldsymbol{G}\boldsymbol{s} & 2\pi^2\boldsymbol{s}^{\mathrm{H}}\boldsymbol{G}^{\mathrm{H}}\boldsymbol{N}^3\boldsymbol{G}\boldsymbol{s} & \pi^2\boldsymbol{s}^{\mathrm{H}}\boldsymbol{G}^{\mathrm{H}}\boldsymbol{N}^4\boldsymbol{G}\boldsymbol{s} \end{bmatrix} \tag{42}$$

4.3. CRLB for stationary and Constant-Envelope signal

The expression in Eq. (42) is signal-specific. For a stationary and constant-envelope signal with power spectral density

$S(f)$, however, we are more interested in the FIM of θ regardless of observation window and signal type. This can be obtained using the expectation of $\boldsymbol{J}_\theta$, which is expressed in Eq. (43).

$$\bar{\boldsymbol{J}}_\theta = E[\boldsymbol{J}_\theta] = \frac{2B_nT}{\sigma_1^2+\sigma_2^2}\int_{-\infty}^{\infty} \times \begin{bmatrix} (2\pi f)^2 & (2\pi f) & 0 & \frac{\pi(B_nT)^2}{(2+1)2^2}(2\pi f) \\ (2\pi f) & 1 & 0 & \frac{\pi(B_nT)^2}{(2+1)2^2} \\ 0 & 0 & \frac{4\pi^2(B_nT)^2}{(2+1)2^2} & 0 \\ \frac{\pi(B_nT)^2}{(2+1)2^2}(2\pi f) & \frac{\pi(B_nT)^2}{(2+1)2^2} & 0 & \frac{\pi^2(B_nT)^4}{(4+1)2^4} \end{bmatrix} S(f)\mathrm{d}f \tag{43}$$

Note that $B_n = 1/T_s$ denotes the noise bandwidth and $\int_{-\infty}^{+\infty} S(f)\mathrm{d}f = 1$ always holds as the power of signal is normalized. For baseband BPSK signal, it also has $\int_{-\infty}^{+\infty} fS(f)\mathrm{d}f = 0$. Therefore, the cross information between TDOA, FDOA and differential Doppler rate is zero, which means that these parameters are estimated without interference. Namely, the TDOA and FDOA low bounds are the same no matter differential Doppler rate is known or not. Furthermore, the low bound of TDOA, FDOA and differential Doppler rate can be given as

$$\mathrm{CRLB}(\tau) = (E[\boldsymbol{J}_{\boldsymbol{\theta}}]^{-1})_{1,1} = \frac{1}{\beta_s^2} \times \frac{1}{B_nT} \times \frac{\sigma_1^2+\sigma_2^2}{2} \tag{44a}$$

$$\mathrm{CRLB}(f_c) = (E[\boldsymbol{J}_{\boldsymbol{\theta}}]^{-1})_{2,2}/T_s^2 = \frac{3}{\pi^2T^2} \times \frac{1}{B_nT} \times \frac{\sigma_1^2+\sigma_2^2}{2} \tag{44b}$$

$$\mathrm{CRLB}(\dot{f}_c) = (E[\boldsymbol{J}_{\boldsymbol{\theta}}]^{-1})_{3,3}/T_s^4 = \frac{180}{\pi^2T^4} \times \frac{1}{B_nT} \times \frac{\sigma_1^2+\sigma_2^2}{2} \tag{44c}$$

where

$$\beta_s^2 = \frac{\int_{-\infty}^{+\infty}(2\pi f)^2 S(f)\mathrm{d}f}{\int_{-\infty}^{+\infty} S(f)\mathrm{d}f} = \int_{-\infty}^{+\infty}(2\pi f)^2 S(f)\mathrm{d}f \tag{45}$$

denotes the root-mean-square bandwidth.

It can be seen from Eqs. (44a) and (44b) that the CRLB of TDOA and FDOA derived from the dynamic signal model in Eq. (11) is the same with that derived from the conventional model in Eq. (1)[15], meaning that there is no accuracy loss on the TDOA and FDOA using the new model. Besides, the CRLB of differential Doppler rate obtained in Eq. (44c) shows that the accuracy of differential Doppler rate is directly related to T^5, meaning that a better differential Doppler rate estimation needs a larger observation window length. The CRLB in Eqs. (44a)–(44c) is useful to evaluate parameter estimation accuracy and forecast location precision. In Section 3.4, the CRLB has been used to evaluate estimation accuracy and in Section 5, it will be further used to compare estimation accuracy in simulations.

5. Simulation analysis

This section contains numerical simulations to demonstrate the proposed method and to evaluate its performance under different conditions.

The first simulation is implemented to evaluate the estimation variance of the proposed method. The assumed emitter signal is a BPSK signal with symbol rate of B = 10 kHz and carrier frequency of f_0 = 400 MHz. The total observation time is T = 0.2732 s and the sampling rate is F_s = 30 kHz. The TDOA is $\tau = 10/F_s$, FDOA is f_c = 520 Hz and differential Doppler rate is $\dot{f}_c$ = 100 Hz/s. It can be deduced that the relative time companding factor is 0.0036 and relative Doppler companding factor is 7.4, so only RDC has to be concerned in our simulation condition. Besides, all the RMSE curves are based on 500 times of Monte Carlo experiments in our simulation.

Fig. 2 shows TDOA estimation RMSE corresponding to SNR. The four plotted curves are statistical RMSE of TDOA using SAF, statistical RMSE of TDOA using compensated CAF, theoretical RMSE of TDOA using SAF, and CRLB of TDOA. It is important to note that the statistical RMSE of TDOA using SAF is obtained by the first step of the proposed method and the RMSE of TDOA using compensated CAF is obtained by the second step of the proposed method, in which the differential Doppler rate has been compensated. The following can be found: (A) The statistical RMSE using SAF is coincident with the theoretical one, meaning that our theoretical analysis of SAF is effective. (B) In both low and high SNR conditions, the RMSE of the compensated CAF can approach the CRLB, meaning that the performance is good. (C) In the low SNR condition, the estimation performance of SAF on TDOA is quite poor while the performance of compensated CAF is much better and it can almost achieve the CRLB. This is because the CAF transform contains less cross items compared with SAF transform, and thus the noise level is not enlarged too much in low SNR condition. Besides, differential Doppler rate is compensated using its estimation value and RDC problem is avoided in the proposed method. The experimental results are consistent with the theoretical analysis in Section 3.4.

Fig. 3 illustrates the FDOA estimation RMSE corresponding to SNR. It can be seen that the estimation of FDOA achieves a significantly good performance under both low and high SNR conditions and it can approach its CRLB. This is because that the differential Doppler rate is compensated in the estimation of FDOA. For example, when SNR = 0 dB, the differential Doppler rate estimation accuracy in the first step is about 1.3 Hz/s and the residual Doppler companding factor is 0.09. This factor is really small enough and can be

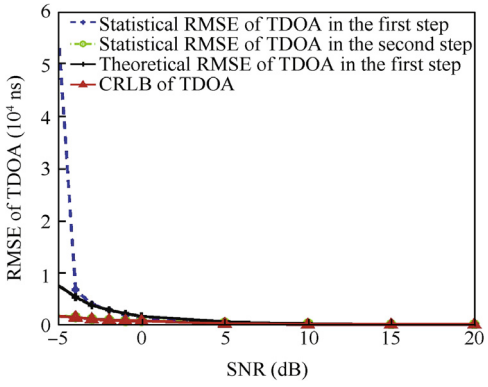

Fig. 2 RMSE of TDOA estimation.

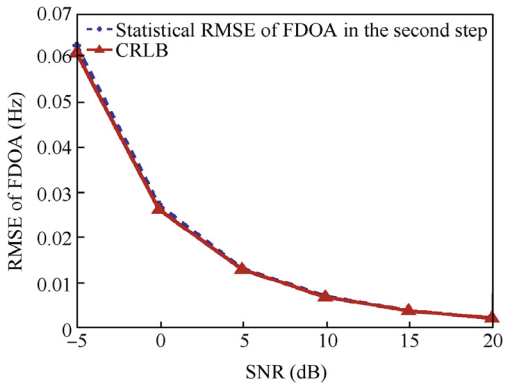

Fig. 3 RMSE of FDOA estimation.

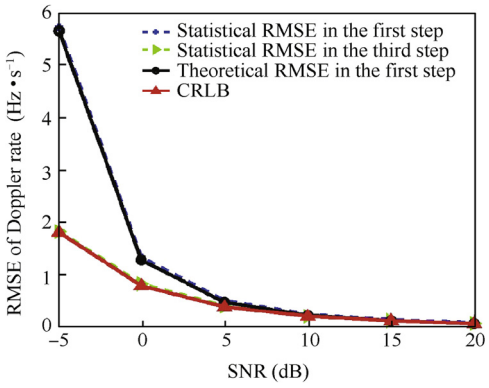

Fig. 4 RMSE curves of differential Doppler rate estimation with lag of $N/4$.

almost ignored. As a result, the accuracy of FDOA can approach its CRLB. The experimental result is accordant with the theoretical analysis.

Fig. 4 demonstrates differential Doppler rate estimation RMSE corresponding to SNR. Four curves are plotted in this figure, including statistical RMSE in the first step, theoretical RMSE in the first step, statistical RMSE in the third step and the CRLB. Note that the estimation of differential Doppler rate in the first step is obtained by SAF and that in the third step is obtained by cross estimator, which is also the final estimation. The following can be found: (1) The differential Doppler rate estimation performance using SAF is poor in the low SNR condition. This is because the SAF transform contains too many cross items and enlarges noise level at low SNR. (2) The statistical RMSE using SAF is in agreement with the theoretical one, indicating that the theoretical analysis is effective. (3) The final Doppler rate estimation performance in the third step is quite well at both low and high SNRs and it can approach the CRLB. This is because the final estimation of differential Doppler rate is obtained using cross estimator and it does not enlarge noise level as SAF. Besides, the estimated TDOA and FDOA used in the third step are accurate enough and have approached CRLB as shown in Figs. 2 and 3, so differential Doppler rate estimation is hardly affected by the above parameters and can also approach CRLB. The experimental results are accordant with our theoretical analysis.

The second simulation is implemented to compare the estimation performance of the proposed method, the conventional CAF method[13] and the ML method[37] using rotating tethered satellite formation. As a new design scheme formation, tethered satellite formation draws great attention in recent years.[6,38] Tethered satellite formation is composed of two or more satellites, which are connected with each other by long tethers. It can be utilized for a variety of space missions and scientific researches.[6] Particularly, the rotating tethered satellite formation can also be used for source localization.[32] In this simulation, we assume that the distance between satellites is 3.75 km, the height from the earth is 500 km and rotation period is 50 s. The FDOA is 520 Hz and the differential Doppler rate is about 300 Hz/s . The assumed emitter signal is the same with that in the previous simulation. It can be deduced that the relative time companding factor is 0.0036 and relative Doppler companding factor is 22.4, so only RDC happens under our simulation condition.

Fig. 5(a) shows a comparison of TDOA estimation. It can be seen that the accuracy of the proposed method is close to that of the ML method and both these two methods can approach CRLB. In contrast, the conventional CAF method performs poorer than the above two methods. This is because the RDC problem reduces the output SNR of CAF, although the CAF's shape in the TDOA direction is not distorted in conventional CAF method. It has to be noted that although our method performs close to ML method, its computational burden is much less. Fig. 5(b) shows a comparison of FDOA estimation. It is clear that the proposed method performs closely to ML method and both of them can approach CRLB, but our method's computational burden is much less. Besides, the accuracy of the proposed method is much better than that of

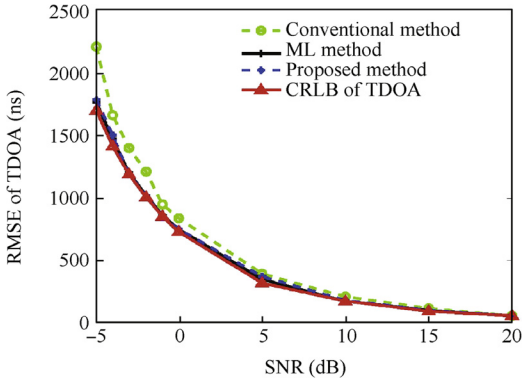

(a) Comparison of TDOA accuracy

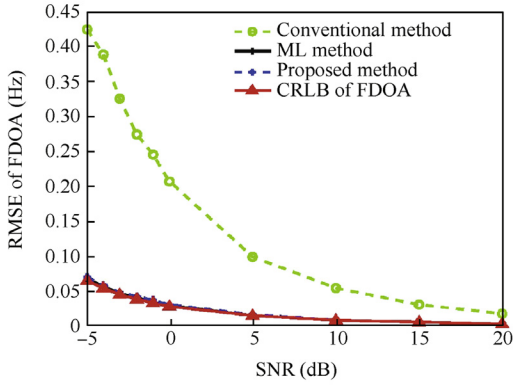

(b) Comparison of FDOA accuracy

Fig. 5 Comparison between proposed method and other methods.

conventional CAF method, increasing by many times. This is because the proposed method can avoid RDC problem, while the conventional method suffers from both the reduction of output SNR and distortion of CAF in FDOA direction. This simulation result is accordant with the theoretical analysis.

6. Conclusions

This paper focuses on RDC problem in the estimation of FDOA, gives a joint estimation method of TDOA, FDOA and differential Doppler rate, derives its CRLB and analyzes the estimation error. The estimation method solves the three-dimensional searching process by two two-dimensional searching and one one-dimensional searching. The simulation results show that the estimation of TDOA, FDOA and differential Doppler rate can achieve their CRLB quite well. The differential Doppler rate can not only avoid RDC problem and improve the estimation performance of TDOA/FDOA in satellite or aircraft based high dynamic scenario, but also supply an additional location parameter for a better accuracy.

Acknowledgement

This study was supported by the National Natural Science Foundation of China (No. 61671273).

Appendix A. Some Details in Derivation of $E[\boldsymbol{J}_\alpha]$

This section contains the derivation of $E[\boldsymbol{J}_\alpha]$ from $\boldsymbol{J}_\theta$. Note that T_s denotes the sampling interval and $B_n = 1/T_s$ denotes the noise bandwidth in the following functions.

$$\begin{aligned} E\left[\boldsymbol{s}^{\mathrm{H}}\boldsymbol{s}\right] &= E\left[\sum_{n=-N/2}^{N/2-1} s^*(n)s(n)\right] \\ &\approx E\left[\frac{1}{T_s}\int_{-T/2}^{T/2} s^*(t)s(t)\mathrm{d}t\right] \\ &= B_n T\int_{-\infty}^{+\infty} S(f)\mathrm{d}f \end{aligned} \tag{A1}$$

$$\begin{aligned} E\left[\boldsymbol{s}^{(1)H}\boldsymbol{s}^{(1)}\right] &= E\left[\sum_{n=-N/2}^{N/2-1} s^{(1)*}(n)s^{(1)}(n)\right] \\ &\approx E\left[\frac{1}{T_s}\int_{-T/2}^{T/2} s^{(1)*}(t)s^{(1)}(t)\mathrm{d}t\right] \\ &= B_n T\int_{-\infty}^{+\infty} (2\pi f)^2 S(f)\mathrm{d}f \end{aligned} \tag{A2}$$

$$\begin{aligned} E\left[\boldsymbol{s}^{\mathrm{H}}\boldsymbol{G}^{\mathrm{H}}\boldsymbol{N}^k\boldsymbol{G}\boldsymbol{s}\right] &= E\left[\sum_{n=-N/2}^{N/2-1} n^k s^*(n)s(n)\right] \\ &\approx E\left[\frac{1}{T_s^{k+1}}\int_{-T/2}^{T/2} t^k s^*(t)s(t)\mathrm{d}t\right] \\ &= \frac{(B_n T)^{k+1}}{(k+1)2^{k+1}}\left[1+(-1)^k\right]\int_{-\infty}^{+\infty} S(f)\mathrm{d}f \\ &= \begin{cases} 0 & k=1,3,5\ldots \\ \dfrac{(B_n T)^{k+1}}{(k+1)2^k}\displaystyle\int_{-\infty}^{+\infty} S(f)\mathrm{d}f & k=2,4,6\ldots \end{cases} \end{aligned} \tag{A3}$$

$$\begin{aligned} E\left[\boldsymbol{s}^{(1)\mathrm{H}}\boldsymbol{G}^{\mathrm{H}}\boldsymbol{N}^k\boldsymbol{G}\boldsymbol{s}\right] &= E\left[\sum_{n=-N/2}^{N/2-1} n^k s^{(1)*}(n)s(n)\right] \\ &\approx E\left[\frac{1}{T_s^{k+1}}\int_{-T/2}^{T/2} t^k s^{(1)*}(t)s(t)\mathrm{d}t\right] \\ &= \begin{cases} 0 & k=1,3,5\ldots \\ -\dfrac{(B_n T)^{k+1}}{(k+1)2^k}\displaystyle\int_{-\infty}^{+\infty} (2\pi f)S(f)\mathrm{d}f & k=2,4,6 \end{cases} \end{aligned} \tag{A4}$$

References

1. Zhu GH, Feng DZ, Xie H, Zhou Y. An approximately efficient bi-iterative method for source position and velocity estimation using TDOA and FDOA measurements. *Sig Process* 2016;**125**:110–21.
2. Cao YL, Peng L, Li JZ, Yang L, Guo FC. A new iterative algorithm for geolocating a known altitude target using TDOA and FDOA measurements in the presence of satellite location uncertainty. *Chin J Aeronaut* 2015;**28**(5):1510–8.
3. Ho KC, Xu W. An accurate algebraic solution for moving source location using TDOA and FDOA measurements. *IEEE Trans Signal Process* 2004;**52**(9):2453–63.
4. Wang G, Li Y, Ansari N. A semidefinite relaxation method for source localization using TDOA and FDOA measurements. *IEEE Trans Veh Technol* 2013;**62**(2):853–62.
5. Zhu GH. Bi-iterative method for moving source localisation using TDOA and FDOA measurements. *Electron Lett* 2014;**51**(1):8–10.
6. Wang D, Huang P, Meng Z. Coordinated stabilization of tumbling targets using tethered space manipulators. *IEEE Trans Aerosp Electron Syst* 2015;**51**(3):2420–32.
7. Wang G, Chen H, Li Y, Ansari N. NLOS error mitigation for TOA-based localization via convex relaxation. *IEEE Trans Wireless Commun* 2014;**13**(8):4119–31.
8. Azaria M, Hertz D. Time delay estimation by generalized cross correlation methods. *IEEE Trans Acoust Speech Signal Process* 1984;**32**(2):280–5.
9. Jacovitti G, Scarano G. Discrete time techniques for time delay estimation. *IEEE Trans Signal Process* 1993;**41**(2):525–33.
10. Hu D, Huang Z, Lu JH, Liang K. Time delay estimation based on bandpass sampling theorem and bisection searching. *12th IEEE international conference on fuzzy systems and knowledge discovery (FSKD)*; 2016 Jan 16; Zhangjiajie, China. Piscataway: IEEE Press; 2015. p. 1997–2001.
11. Fowler ML, Hu X. Signal models for TDOA/FDOA estimation. *IEEE Trans Aerosp Electron Syst* 2008;**44**(4):1543–50.
12. Carter GC. Coherence and time delay estimation. *Proc IEEE* 1987;**75**(2):236–55.
13. Stein S. Algorithms for ambiguity function processing. *IEEE Trans Acoust Speech Signal Process* 1981;**29**(3):588–99.
14. Goh SS, Goodman TNT, Shang F. Joint estimation of time delay and Doppler shift for band-limited signals. *IEEE Trans Signal Process* 2010;**58**(9):4583–94.
15. Yeredor A, Angel E. Joint TDOA and FDOA estimation: A conditional bound and its use for optimally weighted localization. *IEEE Trans Signal Process* 2011;**59**(4):1612–23.
16. Shin DC, Nikias CL. Complex ambiguity functions using nonstationary higher order cumulant estimates. *IEEE Trans Signal Process* 1995;**43**(11):2649–64.
17. Rihaczek AW. Delay-Doppler ambiguity function for wideband signals. *IEEE Trans Aerosp Electron Syst* 1967;**3**(4):705–11.
18. Hack DE, Patton LK, Himed B. Detection in passive MIMO radar networks. *IEEE Trans Signal Process* 2014;**62**(11):2999–3012.

19. Betz J. Effects of uncompensated relative time companding on a broad-band cross correlator. *IEEE Trans Acoust Speech Signal Process* 1985;**33**(3):505–10.
20. Ulman R, Geraniotis E. Wideband TDOA/FDOA processing using summation of short-time CAF's. *IEEE Trans Signal Process* 1999;**47**(12):3193–200.
21. Betz J. Comparison of the deskewed short-time correlator and the maximum likelihood correlator. *IEEE Trans Acoust Speech Signal Process* 1984;**32**(2):285–94.
22. Yasotharan A, Thayaparan T. The performance of the Fourier method in detecting an accelerating target and estimating its median velocity. *2000 IEEE Radar Conference*; 2016 May 12; Alexandria(VA), USA. Piscataway: IEEE Press; 2000. p. 59–64.
23. Hu D, Huang Z, Chen X, Lu J. A moving source localization method using TDOA, FDOA and doppler rate measurements. *IEICE Trans Commun* 2016;**99**(3):758–66.
24. Diao M, Wang Y. Research of passive location based on the Doppler changing rate. *Syst Eng Electron* 2006;**5**:015.
25. Rose CM. Doppler rate and angle rate passive emitter location. U.S. Patent 5689274. 1997-11-18.
26. Xu J, Yu J, Peng YN, Xia XG. Radon-Fourier transform for radar target detection, I: Generalized Doppler filter bank. *IEEE Trans Aerosp Electron Syst* 2011;**47**(2):1186–202.
27. Xu J, Xia XG, Peng SB, Yu J, Peng YN. Radar maneuvering target motion estimation based on generalized Radon-Fourier transform. *IEEE Trans Signal Process* 2012;**60**(12):6190–201.
28. Xu J, Yu J, Peng YN, Xia XG. Radon-Fourier transform for radar target detection (II): Blind speed sidelobe suppression. *IEEE Trans Aerosp Electron Syst* 2011;**47**(4):2473–89.
29. Xu J, Zhou X, Qian LC, Xia XG, Long T. Hybrid integration for highly maneuvering radar target detection based on generalized radon-fourier transform. *IEEE Trans Aerosp Electron Syst* 2016;**52**(5):2554–61.
30. Qian LC, Xu J, Xia XG, Sun WF, Long T. Fast implementation of generalised Radon-Fourier transform for manoeuvring radar target detection. *Electron Lett* 2012;**48**(22):1427–8.
31. Yu J, Xu J, Peng YN, Xia XG. Radon-Fourier transform for radar target detection (III): Optimality and fast implementations. *IEEE Trans Aerosp Electron Syst* 2012;**48**(2):991–1004.
32. Zhang S, Huang Z, Hu D. Investigation on source localization performance using rotating tethered satellite formation. *2016 8th international conference on wireless communications & signal processing (WCSP)*; 2016. p. 1–5.
33. Scaglione A, Barbarossa S. Statistical analysis of the product high-order ambiguity function. *IEEE Trans Inf Theory* 1999;**45**(1):343–56.
34. Barbarossa S, Scaglione A, Giannakis GB. Product high-order ambiguity function for multicomponent polynomial-phase signal modeling. *IEEE Trans Signal Process* 1998;**46**(3):691–708.
35. Porat B, Friedlander B. Asymptotic statistical analysis of the high-order ambiguity function for parameter estimation of polynomial-phase signals. *IEEE Trans Inf Theory* 1996;**42**(3):995–1001.
36. Kay SM. Fundamentals of statistical signal processing, volume I: estimation theory. Upper Saddle River (NJ): Prentice Hall; 1993.
37. Borowiec K, Malanowski M. Accelerating rocket detection using passive bistatic radar. *17th International IEEE Radar Symposium (IRS)*; 2016. p. 1–5.
38. Chang I, Park SY, Choi KH. Nonlinear attitude control of a tether-connected multi-satellite in three-dimensional space. *IEEE Trans Aerosp Electron Syst* 2010;**46**(4):1950–68.